Converted-wave seismic exploration: An update

Robert R. Stewart

ABSTRACT

Multicomponent seismic recording (measurement with vertical- and horizontal-component geophones and possibly a hydrophone or microphone) captures the seismic wavefield more completely than conventional single-element techniques. Multicomponent surveying has developed rapidly, allowing creation of converted-wave or *P-S* images. *P-S* imaging uses downgoing *P* waves that convert on reflection, only at their deepest point of penetration, to upcoming *S* waves. Current *P-S* sections are approaching (and in some cases exceeding) the quality of conventional *P-P* seismic data. The advancements in multicomponent seismic acquisition, processing, and interpretation techniques have led to a number of applications for converted-wave surveys. Uses that have arisen include structural imaging (e.g., "seeing" through gas-bearing sediments; improved fault definition; enhanced near-surface resolution), lithologic estimation (e.g., sand versus shale content; porosity), anisotropy analysis (e.g., fracture density and orientation), subsurface fluid description, and reservoir monitoring.

INTRODUCTION

The reflection seismic technique has been remarkably successful in providing subsurface images over a wide range of depths and environments. The method has been especially useful in the search for hydrocarbons in sedimentary basins, but has also found application in hardrock regions (Eaton et al., 2003). The history of development of the seismic method includes: 1) acquiring more and higher-fidelity measurements of vibrations induced in the ground, 2) making ever better calculations about how these seismic waves propagate, and 3) improving our inferences about what the resultant pictures mean in terms of rock and fluid properties. As part of the ongoing refinement of the method, we must take into account the elastic nature of Earth materials and the vector reality of the seismic survey. After as full an analysis as possible of the compressional (*P-P*) wavefield (perhaps including attribute, AVO, and anisotropy analysis, pre-stack depth migrations, and inversions), we still may not have an adequate image or understanding of our subsurface target.

We can extend the conventional single-sensor method of analysing *P*-waves to include more measurements (horizontal sensors in addition to the vertical geophone or hydrophone) for recording the full vector seismic wavefield. This multicomponent seismic method, now using three or four sensors, has the potential to record many more wavetypes - in particular converted-waves that may tell us more about the target (Stewart et al., 2002; 2003). The simplest, and usually most energetic, converted-wave is composed of *P*-energy propagating downward, converting upon reflection to an upcoming *S*-wave (Figure 1). In isotropic materials, the conversion point is shifted toward the receiver - closer as V_P/V_S increases. However, if the Earth displays vertical transverse isotropic (that is, VTI where velocity varies with angle from the vertical, but not around the vertical), then the conversion point can be displaced toward the mid-point (Thomsen, 1999; Garotta et al., 2003). Most multicomponent processing companies provide VTI assessment as a routine service (as well as analysis of horizontal transverse isotropy, HTI, where the velocity varies with azimuth).

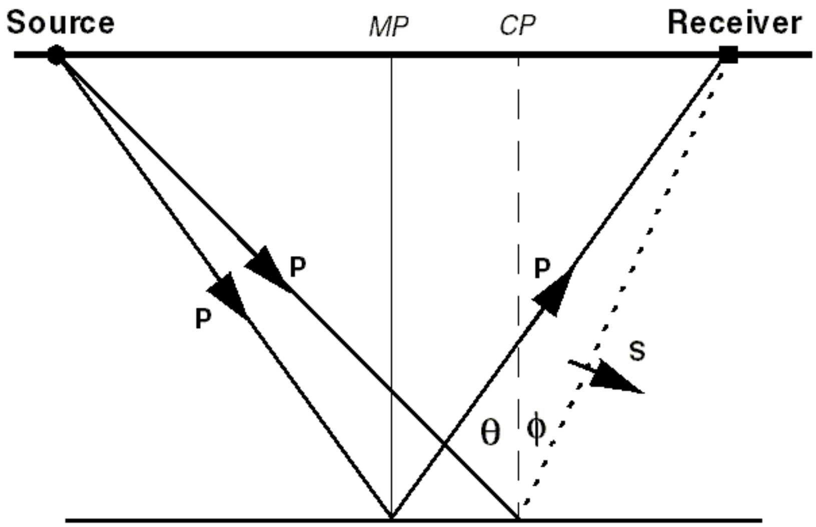

FIG. 1. A converted-wave (*P-S*) reflection at its conversion point (CP) compared to a pure *P*-wave reflection at its midpoint (MP) in an isotropic layer (from Stewart et al., 2002). Note the CP is shifted toward the receiver. The *P*-wave angle of incidence and *S*-wave angle of reflection are given by θ and Φ respectively. Snell's Law gives the relationship between the layer's velocities and the ray angles: $\frac{\sin\theta}{V_P} = \frac{\sin\phi}{V_S}$, where V_P and V_S are the *P*- and *S*-wave velocities, respectively. Since $V_S < V_P$, Φ is less than θ, and the *S*-wave leaves the interface closer to perpendicular than the incident P-wave. Directions of positive phase, as shown by arrowheads, are according to Aki and Richards (1980).

Another aspect of converted-wave propagation is that the reflectivity with offset is quasi-sinusoidal (Figure 2). Generally, we see the amplitude of the conversion fall off to zero at zero offset. However, some careful investigators have noticed that non-zero amplitudes can actually occur at zero offset. Artola et al. (2003) have recently offered theoretical derivations that in certain complicated anisotropic contacts this should occur. Refinements continue. In addition, we usually assume that fluids do not alter the rigidity or *S*-wave velocity of a material substantially. Again though, in fractured and thus anisotropic materials, fluids can change the rigidity considerably. Thus, the *S*-velocity and consequent reflectivity may be changed.

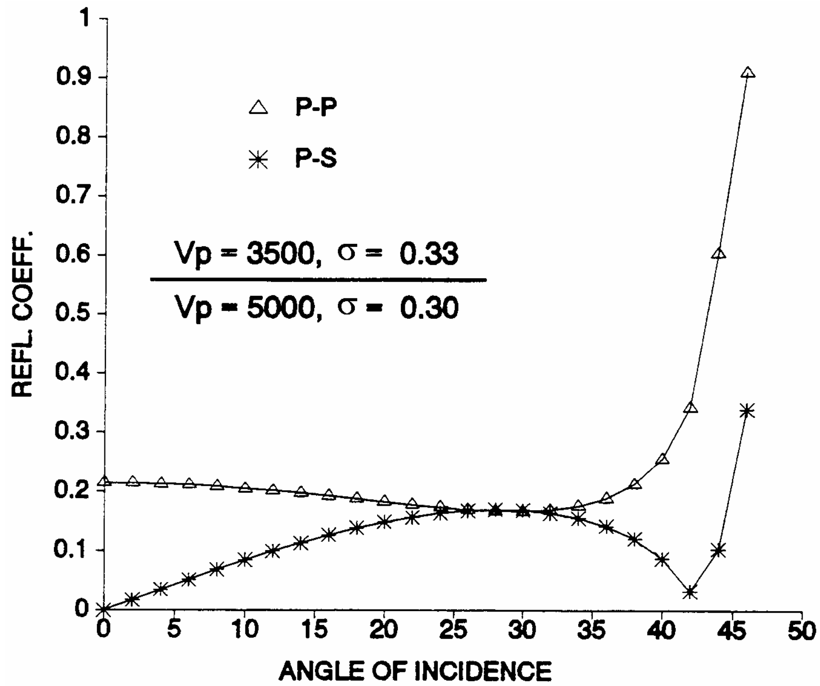

FIG. 2. *P-P* and *P-S* plane-wave reflection coefficients as a function of *P*-wave angle of incidence. Note that the absolute value of the *P-S* reflection coefficient is plotted. The *S*-wave velocities for the upper and lower layers are 1750 m/s and 2650 m/s, respectively. Density is constant (from Stewart et al., 2002).

New digital and optical sensors (e.g., Tessman and Maxwell, 2003; Fischer, 2003) and recording systems promise to provide higher fidelity data, fewer field errors, and greater recording efficiency. Additionally, a number of service companies now have multicomponent seismic capability and growing experience. Survey design codes have been developed and are allowing better designed surveys (e.g., Lawton and Cary, 2003). The economics of multicomponent seismic surveying (Gibson et al., 2003) have been revisited and some costs are improving. Modeling and processing of the elastic wavefields are becoming more and more realistic. Interpretation is taking a leap forward with automatic registration and correlation techniques (Gaiser, 1996; Ogiesoba and Stewart, 2003). Interpretation is stepping forward with specialized elastic-wave interpretation packages such as Hampson-Russell's ProMC.

We would like *S*-waves and their subsequent analysis to provide improved subsurface images as well as give a measure of *S*-wave properties relating to rock type and saturation. If we do have *P-S* reflectivity, what specifically can it be used for? Various authors (e.g., Kristiansen, 2000; Yilmaz, 2001) have suggested or shown a number of applications of *P-S* data that include: enhanced imaging, lithology estimation, fluid description, anisotropy analysis, and reservoir monitoring.

Let's look in more detail at a sample of these applications. First, I will provide an imaging case, then a lithology estimate, follow it with an anisotropy analysis, then a fluid description example, and close with a reservoir monitoring survey.

IMAGING

"Seeing" through gas-charged sediments

P-wave energy is delayed, scattered, and attenuated when passing through a gas-bearing sediment. Leaky gas reservoirs can create a gas plume or chimney that makes conventional *P*-wave imaging and characterization of the reservoir very difficult. *S*-waves, being generally less sensitive to rock saturants, can be used to penetrate gas-saturated sediments. Rodriguez (2000) analysed a 4-C case from the Valhall field, Norway (originally conducted by Amoco Norway Oil Co. and the Valhall Licence partners). He used prestack equivalent-offset migration for converted waves (Bancroft, 2000) to image through a gas cloud. The results provided a more interpretable image of the chalk reservoir beneath the gas cloud, especially near its anticlinal top at about 2.8 s on the *P*-wave section (Figure 3).

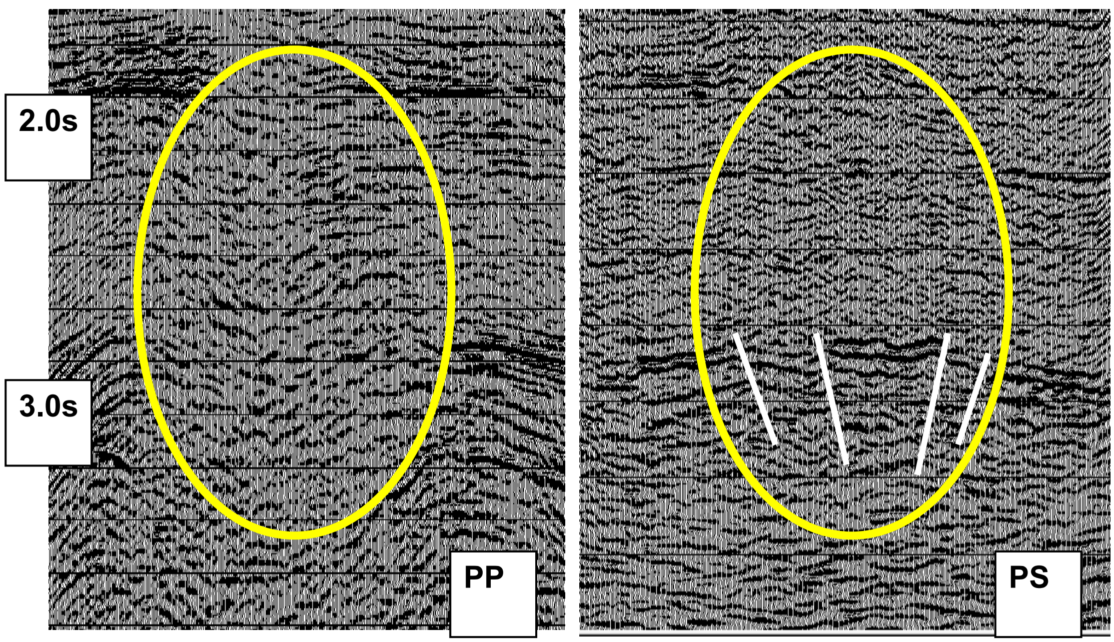

FIG. 3. *P-P* and *P-S* sections from the Valhall field, Norway showing improved imaging across the anticlinal structure (after Rodriguez, 2000). The yellow ellipses outline the upper region of the chalk reservoir.

Structural imaging

Resolution of steeply dipping features can be improved using converted waves in certain circumstances. Purnell (1992) showed examples from physical-modeling data where high-dip anomalies were more visible on migrated *P-S* data than on migrated *P-P* data. Cary and Couzens (2000) gave examples from the Mahogany field in the Gulf of Mexico where *P-S* images show excellent definition of faults associated with salt intrusion (Figure 4). It is not obvious, at this point, why faults should appear to be better defined on the *P-S* versus *P-P* sections. Explanations could include more prominent *P-S* scattering from non-welded or fluid-saturated contacts (Chaisri and Krebes, 2000), larger lateral *S*-wave changes across the faults, or *P-S* raypaths from steeply dipping features that are more conducive to capture with given receiver apertures.

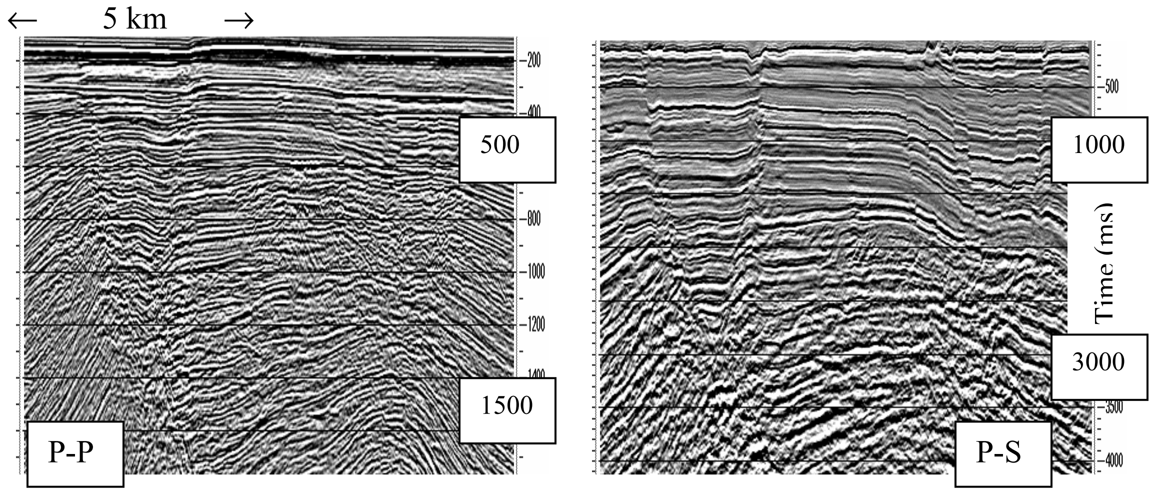

FIG. 4. (a) Poststack time migration of the vertical geophone component from the Mahogany 4-C survey (left). Poststack time migration of the depth-variant CCP stack of the in-line component data on the right (from Cary and Couzens, 2000).

Near-surface imaging

We often see more highly resolved reflectors in the near surface on *P-S* sections than on collocated *P-P* sections. This may be the result of a number of factors, including greater relative changes in *S* versus *P* velocity, a greater impact of density changes on the *P-S* reflectivity than on *P-P* reflectivity, or a shorter *S* wavelength. For example, a 3-C seismic line was acquired over the Steen River impact structure, Alberta by Gulf Canada Resources Ltd. (now ConocoPhillips) in partnership with the CREWES Project at the University of Calgary (Mazur et al., 2002). The resultant *P-P* and *P-S* sections are shown in Figure 5, where the *P-P* data are stretched by a factor of 2 (a V_P/V_S value of 3) to match the *P-S* data. The sections are spliced together at a central point on the line. We note the greater detail evident on the *P-S* sections above the pre-Cretaceous unconformity (at time 1000ms on the *P-S* section). However, the *P-P* data are generally more continuous beneath the pre-Cretaceous unconformity (at about 480 ms on the *P-P* section).

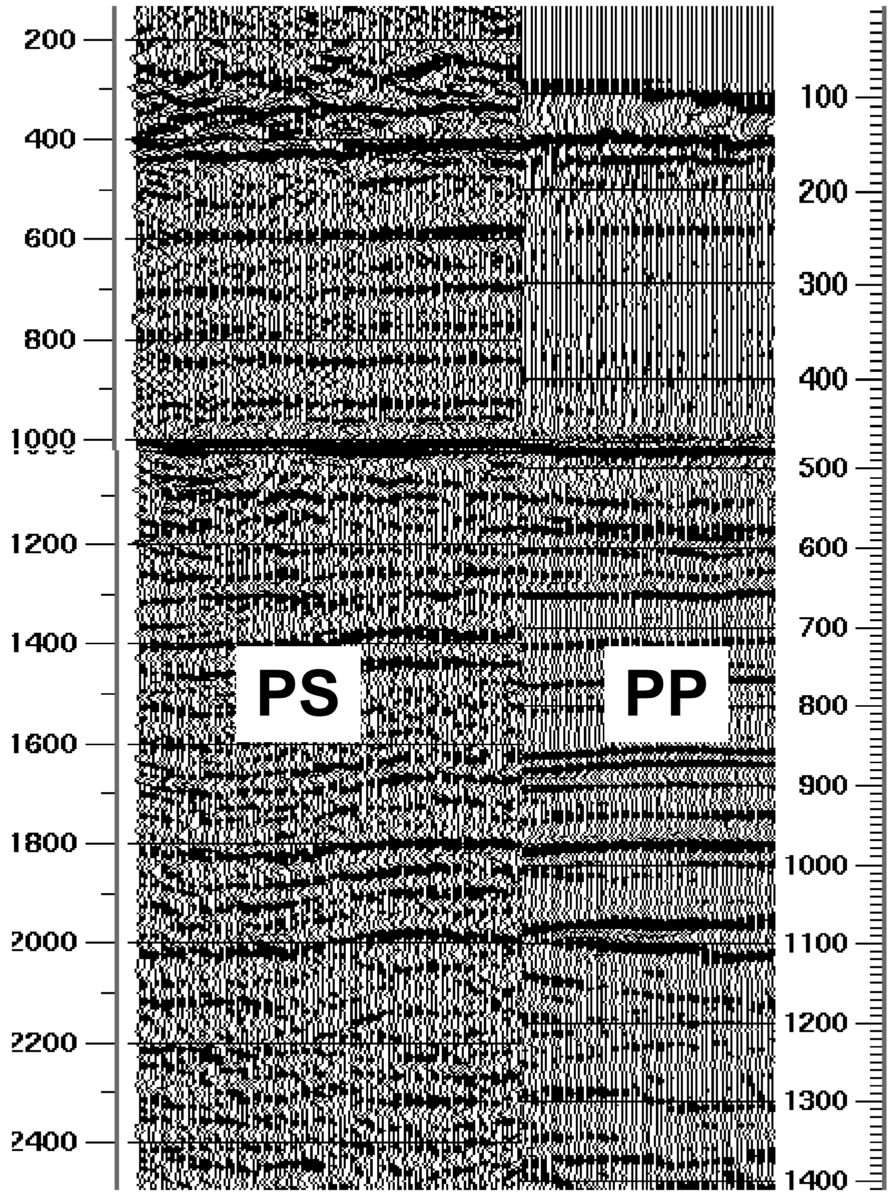

FIG. 5. Seismic data over the Steen River meteorite impact structure, Alberta. The pre-Cretaceous unconformity is expressed at about 480 ms on the *P-P* section and 1000 ms on the *P-S* section. We note that some events are more clearly defined in the shallow *P-S* section, whereas the deeper events are less noisy on the *P-P* section. The data were acquired by Gulf Canada Resources Ltd. (now ConocoPhillips) and the CREWES Project at the University of Calgary.

Richardson (2003) discusses shallow seismic imaging to investigate coal deposits. She notes the importance of fault assessment in coal mine design and the benefits that multicomponent seismic imaging can bring to coalfield understanding. An example of multicomponent surveying to provide enhanced visibility of a coal seam over a coal mine in the Bowen Basin in Australia is shown in Figure 6 (Velseis, 2003).

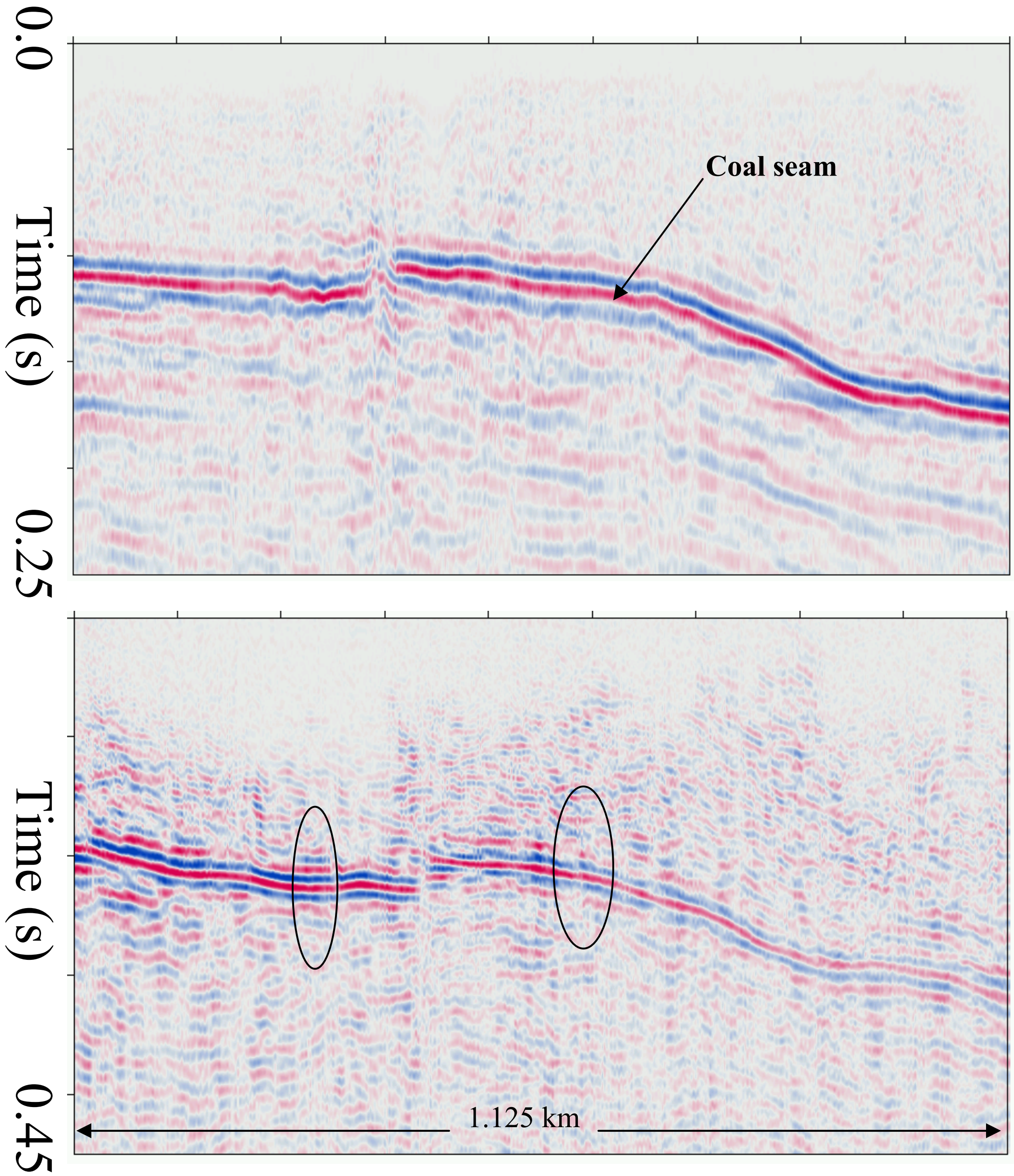

FIG. 6. *P*-wave and converted-wave sections over a faulted coal seam in Australia. The *P-S* and *P-P* sections are in their raw two-way vertical traveltimes, but the *P-S* section has been squeezed to provide an approximate correlation with the *P-P* section. The *P-S* section appears somewhat more resolved than the *P-P* image in addition to its indication of further faulting as shown in the annotated ovals (after Velseis, 2003).

LITHOLOGY ESTIMATION

Sand/Shale

P-wave imaging has proven particularly adept at making structural pictures of the subsurface; that is, providing an image of strata interfaces in reflection time. However, beyond the configuration of interfaces, we would like to know what kind of rock and fluids are in the section. *P*-wave images may be limited or ambiguous in these regards. *S*-wave measurements provide additional constraint on the rock properties (especially on density and rigidity contrasts). Much *P-S* analysis is targeted at finding an *S*-wave velocity or determining a V_P/V_S value (*e.g.*, Li et al., 1999). Both V_S and V_P/V_S can be good indicators of rock type, especially in combination with V_P (Tatham, 1982).

A series of seismic experiments in the Blackfoot oil field, Alberta was conducted to identify sand reservoir facies from non-reservoir rocks (Stewart et al., 1996; Dufour et al., 2002). The surveys included broad-band 3C-2D data, 3C-3D data, and 2-D and 3-D VSP surveys. The field was originally discovered and developed using *P*-wave amplitude anomalies (Figure 7a); however, there are also amplitude anomalies not associated with sand channels (that is, false positives). *P-P* isochron maps are also indicative of the channel but again with some ambiguity.

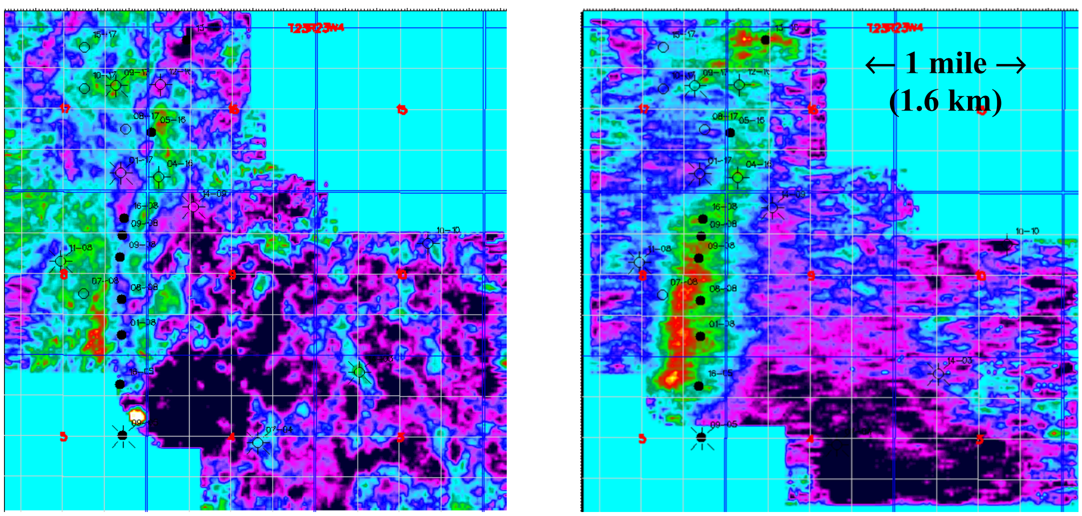

(a) (b)

FIG. 7. (a) *P-P* time slice at the interpreted sand channel level from the Blackfoot 3C-3D survey (the channel is interpreted to be the purple N-S feature) and (b) *P-S* associated time slice. The grid lines indicate a section (1 mile by 1mile or approximately 1.6 km by 1.6 km).

Modelling, VSP surveys in the area, and a 2D-3C seismic line over the middle of the main pool all indicated promise for *P-S* images to reduce the ambiguity. So, a 3C-3D survey was conducted. The resultant *P-S* amplitude seems to give a more definitive (but lower resolution) image of the sand channel (Figure 7b). A *P-S* isochron map that included the channel is perhaps more compelling (Figure 8a). The V_P/V_S maps, calculated from *P-P* and *P-S* isochron map ratios, are another strong indicator of the reservoir sand channel trend (Figure 8b).

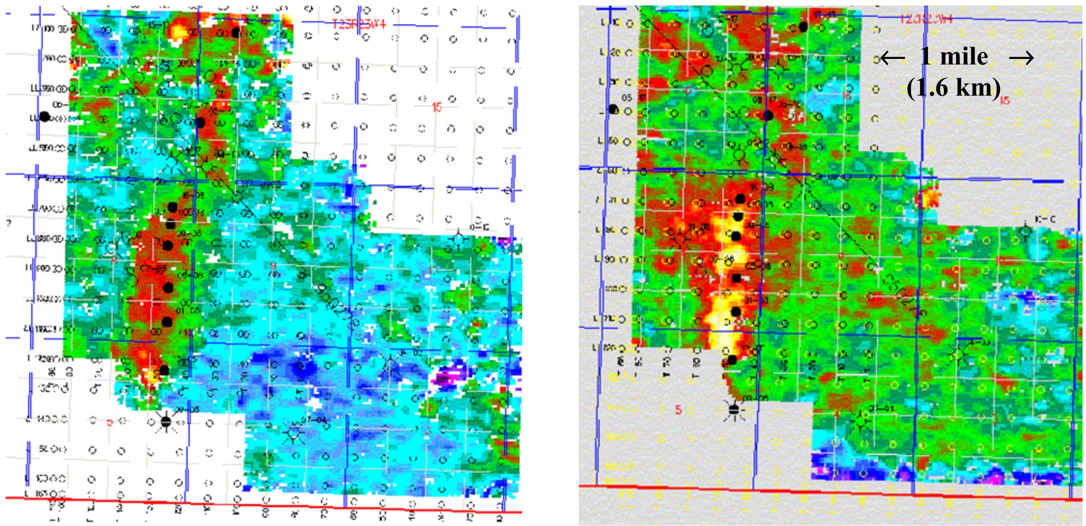

(a) (b)

FIG. 8. (a) *P-S* isochron map between the Mannville and Mississippian horizons (white/yellow indicate a time thickness of 140 ms through purple with a value of 90 ms) and (b) the V_P/V_S value as determined from the *P-P* and *P-S* isochron maps between the interpreted top of the channel and Wabamun horizons. White/yellow represent a V_P/V_S value of 1.5 through purple indicating a value of 2.8.

MacLeod et al. (1999a) showed a case (now a classic!) of converted waves successfully delineating sand channels encased in shale at the Alba field in the North Sea. A strong contrast in *S*-wave velocity (from shale to sand) is associated with the top of the reservoir. On the other hand, there is relatively little *P*-wave velocity change across this lithologic boundary. Thus, the reservoir top generates strong converted-waves, but weaker reflected *P*-waves.

The impact of the 4-C OBC survey on the development of Alba has been positive (MacLeod, et al., 1999b). To date, a number of successful wells have been drilled based primarily on the interpretation of the new converted-wave data. Wilkinson (2003, pers. comm.) indicated that up to 100 million barrels of oil had been added to the estimate of the Alba field on the basis of the converted-wave assisted interpretation.

ANISOTROPY ANALYSIS

Many hydrocarbon reservoirs are fractured. The volume of oil or gas in place and the reservoir's ability to produce it can be dependent on the fracture state of the reservoir. Determining fracture density and orientation from seismic data has thus been a subject of considerable effort (e.g., Probert et al. 2000; Crampin, 2001).

Gaiser et al. (2002) showed the results of applying an Alford (1986) anisotropic rotation procedure and layer stripping (where off-diagonal components are minimized) to data from a 4C-3D seismic survey conducted over the Emilio field in the Adriatic Sea, Italy. They found that *S*-wave splitting was in evidence and the fast *S*-wave was polarized in the NNW-SSE direction, which was consistent with faulting in the area (Figure 9).

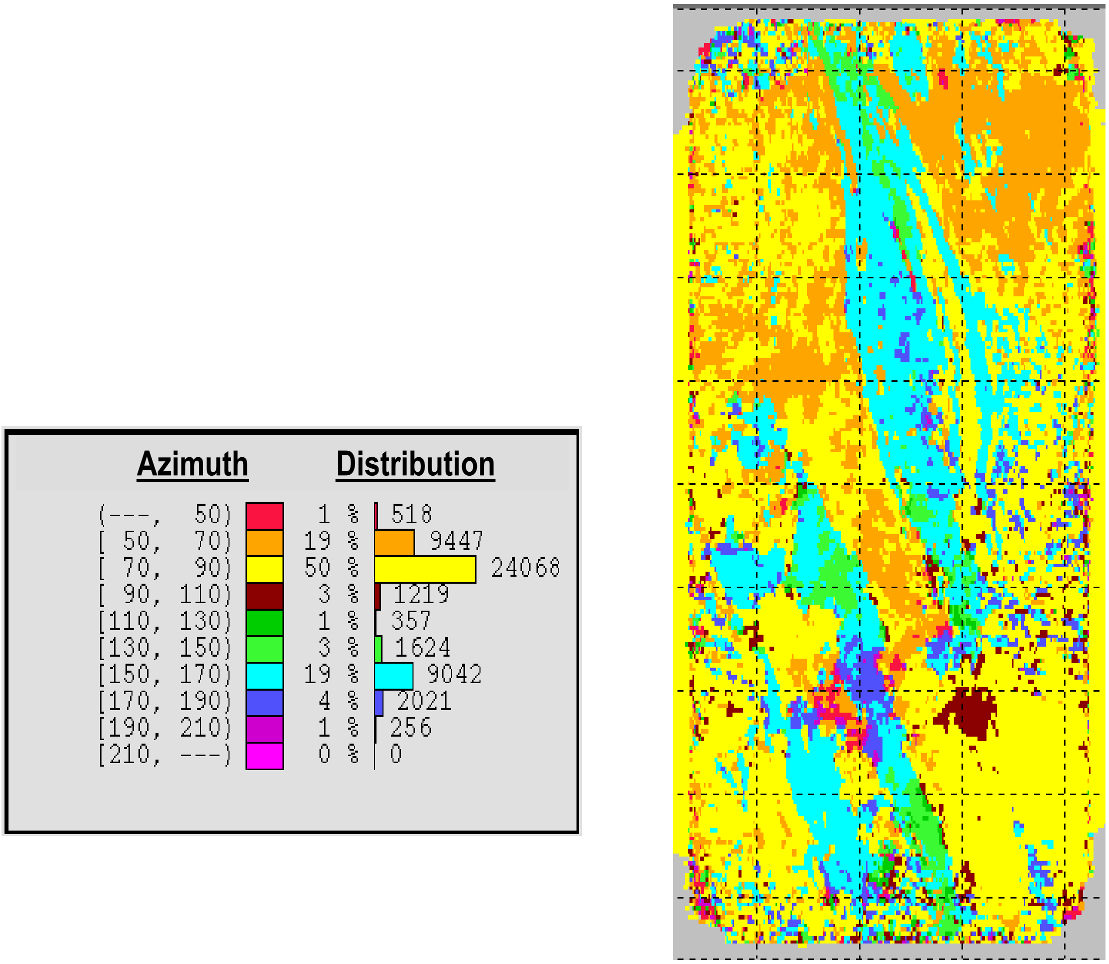

FIG. 9. Fast S polarization direction from a 4C-3D seismic survey over the Emilio field, offshore Italy. Major fracture and faulting trends are NNW-SSE in the regions of interest as are the fast S polarizations (Gaiser et al., 2002).

Numerical modeling (Li et al., 1996) suggests that gas-saturated and oriented fractures may have an effect on anisotropic *P-S* reflectivity. This is in contrast to the isotropic case, where fluid saturation appears to have less impact on *S*-wave velocities. In fact, Guest et al. (1998) interpreted anomalies in *S*-wave splitting over a gas reservoir in Oman as evidence of an effect of gas on shear waves.

FLUID DESCRIPTION

Thompson et al. (2000) presented early results from a 30 km 2-D multicomponent line, in 750 m of water, shot over the Fles Dome, offshore Norway. There is a flat spot on the *P-P* data set that could be an event caused by a fluid contact (Figure 10). However, it could also be generated by a lithologic change. The continuity of dipping strata in the *P-S* section (lack of a flat spot) supports the possibility that the *P-P* anomaly is caused by fluids, not a lithologic change.

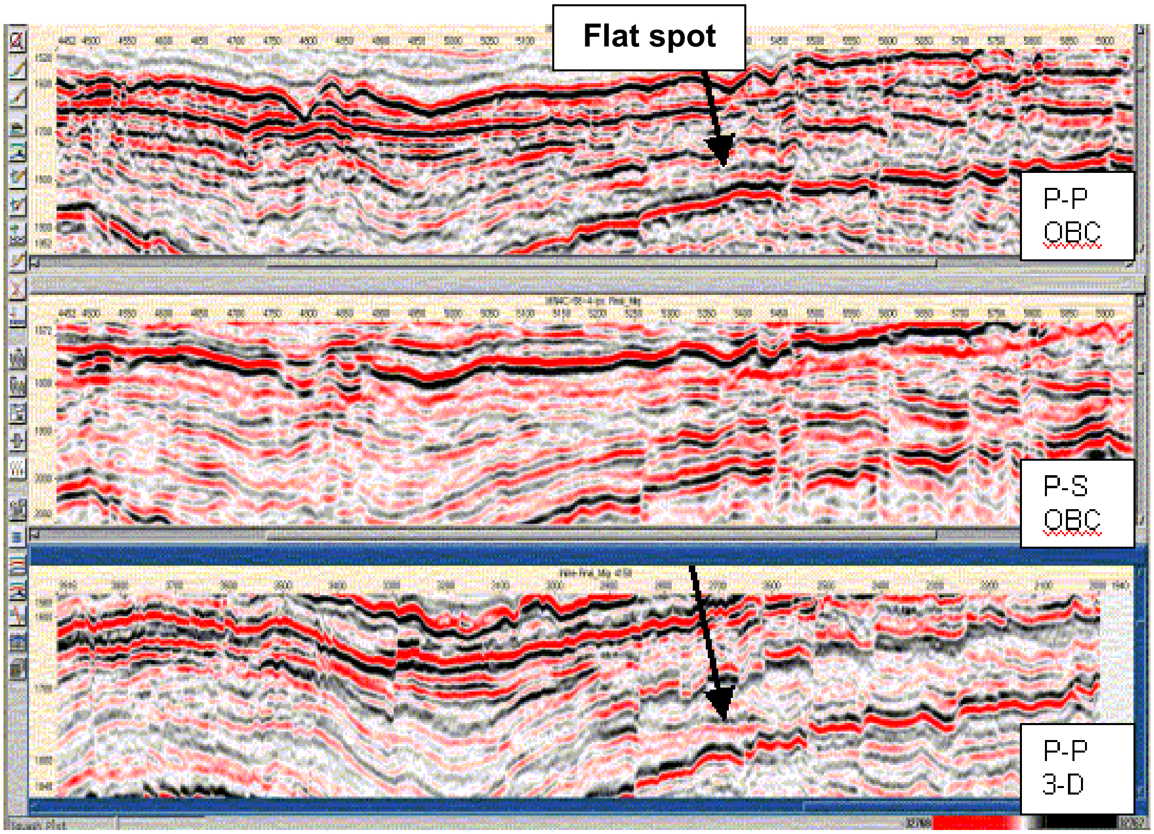

FIG. 10. Flat spot analysis on *P-P* and *P-S* from the Fles prospect, offshore Norway (Thompson et al., 2000). The top section shows the *P*-wave data from the 2-D OBC survey, the middle section the *P-S* data from the OBC survey, and the bottom section a line extracted from a 3-D towed streamer volume. There is no obvious flat spot on the *P-S* data suggesting that the *P*-wave anomaly is a fluid contact not a lithology change.

RESERVOIR MONITORING

Isaac (1996) showed *P-P* and *P-S* sections from a heavy-oil reservoir at Cold Lake, Alberta undergoing steam flooding (Figures 11a and 11b). There are variations in the reservoir rock properties associated with temperature and saturation changes. These, in turn, are associated with changes in the seismic character of both *P-P* and *P-S* sections. Using surveys in 1993 and repeated in 1994, she found that the variation in V_P/V_S values correlated with the temperature of the reservoir. The V_P/V_S values stay fairly constant in areas away from the injection wells (CDPs 20-70 in Figures 12a and 12b). However, in the areas steamed in 1994, there is an increase in V_P/V_S that causes the ratio of the V_P/V_S values from the two years to drop (Figure 12c).

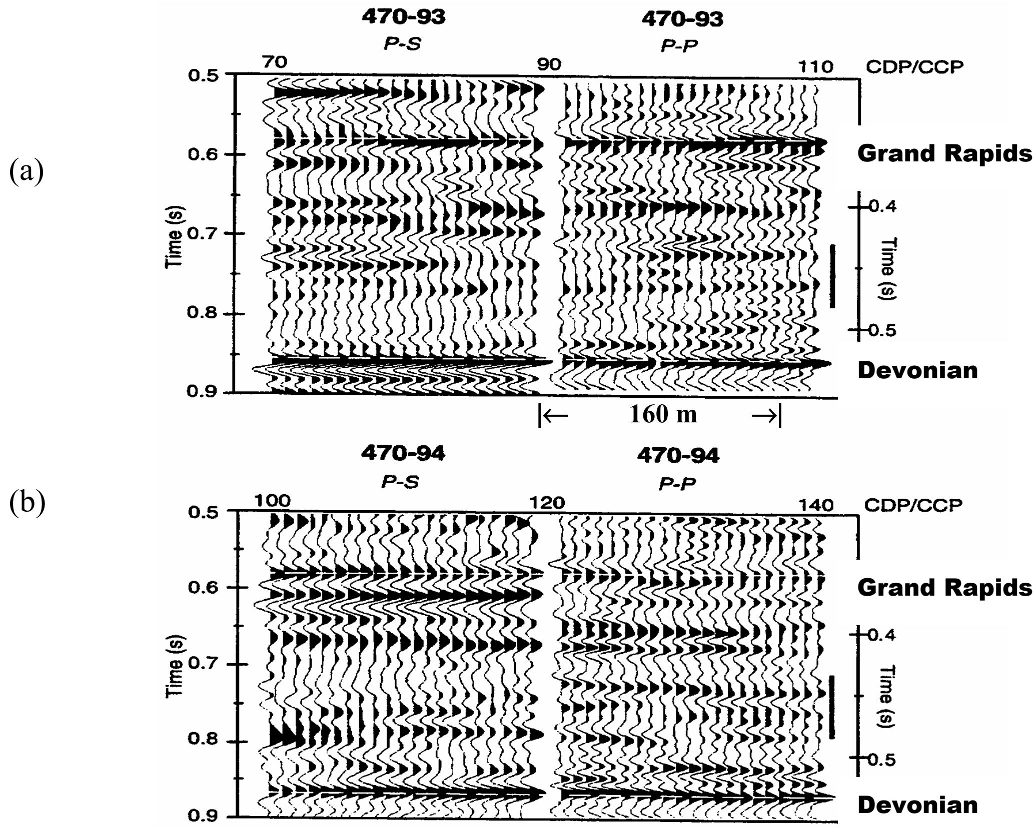

FIG. 11. Comparison of the (a) 1993 and (b) 1994 3-C seismic lines from the Cold Lake, Alberta steam injection site. Note the similar data quality and resolution among all lines (from Isaac, 1996). The area of interest is indicated by the vertical bar. CDP/CCP trace spacing is 8 m.

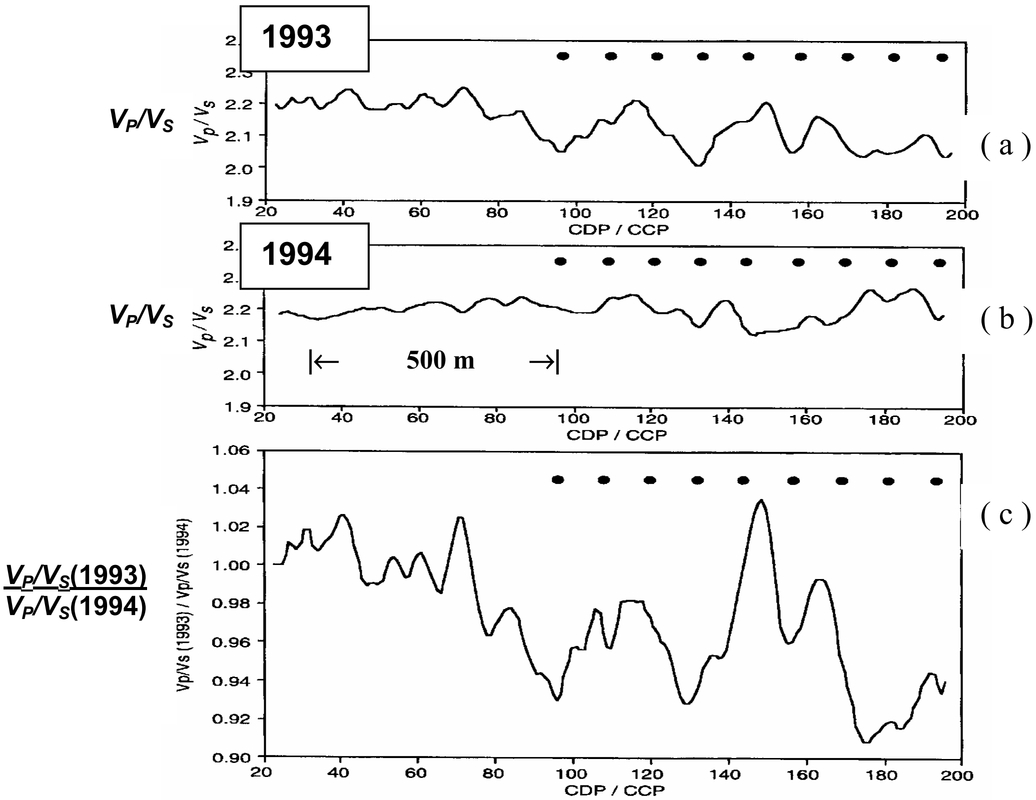

FIG. 12. V_P/V_S plots for (a) 1993 lines, (b) 1994 lines, and (c) the ratio of those two. Note that the V_P/V_S value is fairly constant in the unsteamed regions away from the wells – CDP numbers 20-70 (from Isaac, 1996). However, the V_P/V_S values increase in 1994, with steaming. CDP/CCP trace spacing is 8 m. The lines were 1800 m long.

WHAT'S LEFT TO DO

Converted-wave exploration has come a long way in recent years, but there is still plenty of room for progress. The *P-S* method will undoubtedly become more widely practised and useful as costs decrease. The expense of land multicomponent surveys is decreasing significantly, but marine costs are still well above those of towed-streamer methods. Processing and analysis of *P-S* data have become much more effective and sophisticated, especially by incorporating prestack techniques and anisotropy. Seismic theory has much more to teach us – for example, about non-linear wave propagation. Processing *P-P* and *P-S* data together to provide consistent images in depth (Mikhailov et al., 2001) and improved rock property estimates (Margrave et al., 2001) are critical current developments. For example, Spitz (2001) showed a case from the North Sea where *P-P* and *P-S* inversion was used to derive a density estimate (which compared favourably with a density log in their area). Further refinements await.

More detailed analysis of existing images may provide us with greater understanding of the targets under consideration or even new ones. Better interpretation tools are under development, especially with respect to correlation and depth conversion, but additional advances would be welcomed. Continued education and experience will further unravel what converted waves have to show us (Cary, 2001).

Looking farther ahead, we anticipate making use of other modes that propagate in a seismic survey – such as a wave, otherwise *P*, that has an *S*-wave leg through a high-velocity region. In cases where there are high-velocity layers – basalts, carbonates, salts, or even permafrost in the near surface – seismic imaging may be complicated or compromised.

The possibility of high-quality, fully elastic and anisotropic images of the subsurface opens many doors to new interpretation. Accurately repeating these surveys (4C-4D) to look for changes associated with fluid movement is a very exciting prospect (Grechka, 2001; Jack, 2001). Permanent seismic monitoring of oilfields, either with active sources or passive listening, using surface and/or borehole measurements will provide considerably more guidance for reservoir production.

And even farther out on the horizon, we are beginning to see the imaging use of other kinds of energy conversions (e.g., seismic to electromagnetic). Multicomponent seismic recording with electric and magnetic field sensors may provide estimates of Earth properties that are more closely tied to subsurface fluids.

CONCLUSIONS

The reflection seismic method has used *P*-waves for many years – and with great success. The extension of the reflection method to include *P-S* waves has been effective in yielding new cases of improved imaging of resource targets. Particularly well documented cases exist for gas-cloud imaging, sand/shale discrimination, and anisotropy analysis. There is more to be done in converted-wave exploration seismology, especially in making full use of these new pictures.

ACKNOWLEDGMENTS

I would like to express my deep appreciation to the sponsors of the Consortium for Research in Elastic Wave Exploration Seismology (the CREWES Project) for their commitment to the development of multicomponent seismology. Chris Thompson, formerly of Chevron, graciously donated the Fles example, and the Amoco (now BP) group of companies provided the Valhall 4-C data set for analysis.

REFERENCES

Aki, K. and Richards, P.G., 1980, Quantitative seismology: Theory and methods: W.H. Freeman and Sons, Vols. 1 and 2.

Alford, R.M., 1986, Shear data in the presence of azimuthal anisotropy: Dilly, Texas, 56th Ann. Internat. Mtg., Soc. Expl. Geophys., Houston, S9.6, 476-479.

Artola, F. V.A., Leiderman, Fontoura, S.A.B., and Siva, M.B.C., 2003, Zero-offset C-wave reflectivity in horizontally layered media: Presented at the 73rd Ann. Intl. Soc. Explor. Geophys. Meeting.

Bancroft, J.C., 2000, A practical understanding of pre- and post-stack migration: Vol. 2, Course Note Series, Soc. Explor. Geophys.

Cary, P.W., 2001, Multicomponent seismic exploration in Canada – One person's perspective: Recorder, Can. Soc. Explor. Geophys., **26**, 62-67.

Cary, P.W. and Couzens, R.A., 2000, Processing 4-C data from Mahogany Field, Gulf of Mexico: Presented at the SEG/EAGE Summer Research Workshop, Boise, Idaho.

Chaisri, S. and Krebes, E.S., 2000, Exact and approximate formulas for *P-SV* reflection and transmission coefficients for a nonwelded contact interface: J. Geophys. Res., **105**, 28,045-28,054.

Crampin, S., 2001, Shear-wave anisotropy: A new window into the crack-critical rockmass: Recorder, Can. Soc. Explor. Geophys., **26**, 11-27.

Dufour, J, Squires, J., Goodway, W.N., Edmunds, A., and Shook, I., 2002, Integrated geological and geophysical interpretation case study, and Lamé rock parameter extractions using AVO analysis on the Blackfoot 3C-3D seismic data, southern Alberta, Canada: Geophysics, **67**, 27-37.

Eaton, D.W., Milkereit, B., and Salisbury, M.H., Eds., 2003, Hardrock seismic exploration: Soc. Explor. Geophys., Geophys. Dev. Series, no. 10.

Fischer, P.A., 2003, What's new in sensor technology: World Oil, Gulf Publ. Co., **224**, 9, 29-34.

Gaiser, J.E., 1996, Multicomponent *Vp/Vs* correlation analysis: Geophysics, **61**, 4, 1137-1149.

Gaiser, J.E., Loinger, E., Vetri, L., Lynn, H., and Walters, R., 2002, *PS*-wave birefringence analysis at the Emilio field for fracture characterization: Presented at the 10th Intl. Workshop Seis. Aniso.

Garotta, R., Granger, P.-Y., and Audebert, F. 2003, About gamma ratios and their combinations: Presented at the 73rd Ann. Intl. Soc. Explor. Geophys.

Gibson, J., Watt, H., and Roche, S., 2003, Multicomponent seismic data acquisition… The economics revisited: CSEG Recorder, **28**, 8, 16-21.

Grechka, V., 2001, Seismic anisotropy: Yesterday, today, tomorrow: Recorder, Can. Soc. Explor. Geophys., **26**, 9-10.

Guest, S., Vander Kolk. C., and Potters, H., 1998, The effect of fracture filling fluids on shear-wave propagation: Presented at 68th Ann. Intl. SEG Mtg., Expd. Abst., 948-951.

Isaac, J.,H, 1996, Seismic methods for heavy oil reservoir monitoring: Ph.D. thesis, Univ. of Calgary.

Jack, I., 2001, The coming of age for 4D seismic: First Break, **19**, 1, 24-28.

Lawton, D.C. and Cary, P., 2003, Some considerations with *P-S* survey design: Presented at the 73rd Ann. Intl. Mtg., Soc. Explor. Geophys.

Kristiansen, P., 2000, 4 years experience with 4C seismic: what we have learned: Presented at the SEG/EAGE Summer Research Workshop, Boise, Idaho.

Li, X., Kuhnel, T., and MacBeth, C., 1996, Converted-wave AVO and its implications: Extended Abst., 58th Ann. Conf., Euro. Assn. Geosci. Eng., M046.

Li, X., Yuan, J., Ziolkowski, A., and Strijbo, F., 1999, Estimating V_P/V_S ratio from converted waves – a 4C case example: Extended Abst., 61th Ann. Conf., Euro. Assn. Geosci. Eng., P066.

MacLeod, M.K., Hadley, M.J., Reynolds, K.J., and Tura, A., 1999a, Multicomponent analysis of OBC data, 31st Ann. Off. Tech. Conf., Houston, OTC 10940.

MacLeod, M.K., Hanson, R.A., Bell, C.R., and McHugo, S., 1999b, The Alba field ocean bottom cable seismic survey: Impact on development, Off. Euro. Conf., Aberdeen, SPE 56977.

Margrave, G.F., Stewart, R.R., and Larsen, J.A., 2001, Joint *PP* and *PS* seismic inversion: The Leading Edge, **20**, 1048-1052.

Mazur, M.J., Hildebrand, A.R., Hladiuk, D., Schafer, A., Pilkington, M., and Stewart, R.R., 2002, The Steen River crater seismic refraction project: Presented at the 33rd Lunar and Planetary Science Conf., Houston.

Mikhailov, O., Johnson, J., Shoshitaishvili, and Frasier, C., 2001, Practical approach to joint imaging of multicomponent data: The Leading Edge, **20**, 1016-1021.

Ogiesoba, C. and Stewart, R.R., 2003, *Vp/Vs* from multicomponent seismic data and automatic *PS* to *PP* time mapping: Presented at the 73rd Ann. Intl. Mtg., Soc. Explor. Geophys.

Probert, T., Ronen, S., and Bryan, R., 2000, A case study of azimuthal anisotropy analysis from a N. Sea 3D 4C project: Presented at the SEG/EAGE Summer Research Workshop, Boise, Idaho.

Purnell, G.W., 1992, Imaging beneath a high-velocity layer using converted waves: Geophysics, **57**, 1444-1452.

Richardson, S.E., 2003, Multicomponent seismic applications in coalbed methane development, red Deer, Alberta: M.Sc. thesis, Univ. of Calgary.

Rodriguez, C., 2000, Advanced marine methods: Ocean-bottom and vertical cable analyses: Ph. D. thesis, Univ. of Calgary.

Spitz, S., 2001 Seismic analysis with multi-components: Recorder, Can. Soc. Explor. Geophys., **26**, 7, 57-61.

Stewart, R.R., Ferguson, R., Miller, S.L.M., Gallant, E., Margrave, G., 1996, The Blackfoot seismic experiments: Broad-band, 3C-3D, and 3-D VSP surveys: CSEG Recorder, **6**, 7-10.

Stewart, R.R., Gaiser, J.E., Brown, R.J., and Lawton, D.C., 2002, Converted-wave seismic exploration: Methods: Geophysics, **67**, 5, 1348-1363.

Stewart, R.R., Gaiser, J.E., Brown, R.J., and Lawton, D.C., 2003, Converted-wave seismic exploration: Applications: Geophysics, **68**, 1, 40-57.

Tatham, R.T., 1982, V_P/V_S and lithology: Geophysics, **47**, 336-344.

Tessman, D.J. and Maxwell, P., 2003, Full-wave digital seismic recording and the impact of vector fidelity on improved P-wave data: CSEG Recorder, **28**, 8, 22-24.

Thomsen, L., 1999, Converted-wave reflection seismology over inhomogeneous anisotropic media: Geophysics, **64**, 678-690.

Thompson, C., Helgesen, H.K., and Battié, J.E., 2000, 2D-4C seismic exploration data for risk reduction, Fles prospect, offshore Mid-Norway: Presented at the SEG/EAGE Summer Research Workshop, Boise, Idaho.

Velseis, 2003, Investigation of converted-wave seismic reflection for improved resolution of coal structures: Final Report, ACARP Project C10020, 75pp.

Yilmaz, O., 2001, Seismic data analysis: Processing , inversion, and interpretation of seismic data: Soc. Explor. Geophys., Investigations in geophysics, no. 10., vol. 2.